

UDK: 548.73; 549.3: 677.017.5

## Deposition of Copper Sulfide Films on Polyamide Surface

Neringa Petrasauskiene<sup>1</sup>, Edita Paluckiene<sup>1</sup>, Rasa Alaburdaite<sup>1</sup>, Martina Gilic<sup>2,3\*</sup>

<sup>1</sup>Department of Physical and Inorganic Chemistry, Kaunas University of Technology, Radvilenuj 19, LT-50254 Kaunas, Lithuania

<sup>2</sup>Institute of Physics Belgrade, University of Belgrade, Pregrevica 118, Zemun 11080, Serbia

<sup>3</sup>Institut of Experimental Physics, Freie Universität Berlin, Arnimallee 14, 14195 Berlin, Germany

---

### Abstract:

*In this paper, we present a novel and low – cost method for preparing copper sulfide films on polyamide. Non-treated as well as pre-treated PA6 films by 3 different methods (in boiled water; in NaOH solution; in boiled water and then in NaOH solution) were used for the formation of Cu<sub>2</sub>S layers by the sorption-diffusion method. Molten sulfur has been used as a sulfurization agent. The XRD, FTIR, and UV-VIS methods were used to characterize the structural, optical, and electrical properties of samples and to track changes in samples after each treatment stage. The sheet resistance of Cu<sub>2</sub>S layers depends on the pre-treatment method and varied from 7 kΩ/sq to 6 MΩ/sq. The optical band gaps (E<sub>g</sub>) for direct and indirect transitions are determined to be 2.61–2.67 eV and 1.40-1.44 eV, respectively. Furthermore, the optical constants n, k, and σ are determined from UV-VIS measurements.*

**Keywords:** *Thin film; Copper sulfide; Polyamide 6; X-ray diffraction; Optical properties.*

---

## 1. Introduction

Copper sulfides, Cu<sub>x</sub>S, x=1–2, are one of the most important compounds of chalcogenide semiconductor materials due to their low toxicity, versatility, and availability. They can be used as absorbers and p-type semiconductors due to their excellent electrical, optical, and structural properties [1–3]. The electrical conductivity of copper sulfides is decreasing from CuS to Cu<sub>2</sub>S, direct bandgap values vary from 2.2 to 2.9 eV in Cu<sub>2</sub>S, 2.1 eV in Cu<sub>1.8</sub>S, and 1.7 eV in CuS [1,4–6].

Copper sulfides are widely applied as thin films and composite materials with technologically important applications in optoelectronic devices [7,8], sensors [9,10], photocatalysis [11,12], photovoltaic cells [10,13], for high-energy supercapacitors [14,15], battery electrodes [7,16,17], and in biomedical fields [18,19]. Recently, they found application as counter electrodes in quantum dot sensitized solar cells [15,20]. For all these applications, the material must be highly accessible; therefore, it is very important to identify simple and inexpensive production technologies on a large scale.

The deposition of a thin layer of copper sulfide on the surface of an organic polymer is one of the simple ways to obtain electrically conductive films for the manufacture of electronic devices, because they can change properties from a semiconductor to a metal conductor. The ability of a polymer to sorb fine particles from a solution provides

---

\*) **Corresponding author:** martina.gilic@fu-berlin.de (M. Gilic)

opportunities for many novel applications [21]. Once the copper sulfide is deposited on a flexible transparent polymer substrate, the resulting coated polymer may be applicable in many areas: as the conductive substrate for the deposition of metals and semiconductors [22,23]; as room temperature gas sensors [24,25]; in thermoelectric applications [26].

Polyamide (PA6 or polycapromamide, Nylon 6) as a semihydrophilic polymer is capable of absorbing ions or molecules of various electrolytes from aqueous and non-aqueous solutions [27]. Polyamide can be characterized as a polymer with high thermal resistance and good mechanical properties.

Polymers with electrically conductive metal chalcogenide layers on their surface can be prepared by the sorption-diffusion method described in our earlier works [27–29]. According to this method, the surface of a polymer is pre-treated by a solution containing a sulfurization agent and subsequently treated by an aqueous solution of metal salt.

This work presents a new low-cost method for preparing good quality  $\text{Cu}_2\text{S}$  thin films on a modified PA6 surface. The structure of the prepared films is studied by X-ray diffraction (XRD), Fourier transform infrared (FTIR), and UV-VIS spectroscopy. The material (composite) structure and the optical and electrical properties of  $\text{Cu}_2\text{S}$  films are discussed.

## 2. Materials and Experimental Procedures

### 2.1. Materials

Analytical pure reagents and *distilled water* were used to prepare the reactive solutions. All reagents were obtained from Sigma-Aldrich and used as received. Only freshly prepared solutions were used for experiments and were not de-aerated during the experiments.

The polyamide film (PA6) (Tecamid 6, thickness - 500  $\mu\text{m}$ , density - 1.13  $\text{g}/\text{cm}^3$ , surface resistance  $10^{12} \Omega/\text{sq}$ ) used in this study was obtained from Ensinger GmbH (Germany).

### 2.2. Formation of $\text{Cu}_x\text{S}$ thin layers

According to the bibliography [30], the impregnation of copper sulfide on PA6 or other polymers requires a previous treatment process to facilitate its adhesion. For the experiment, non-treated PA6 samples have been used, as well as the ones pre-treated by 3 different methods: boiled in distilled water for 120 min; exposed to 0.1 M NaOH solution for 120 min at 80°C; boiled in distilled water for 120 min and subsequently exposed to 0.1 M NaOH solution for 120 min at 80°C (Table I). All samples were rinsed and air-dried at room temperature, followed by desiccation with  $\text{CaCl}_2$ .

**Tab. I** Sample labelling and experimental conditions of PA6.

Labelling	Experimental conditions
PA6-0	Non-treated
PA6-1	Boiled in distilled water for 120 min
PA6-2	Exposed to 0.1 M NaOH solution for 120 min at 80°C
PA6-3	Boiled in distilled water for 120 min and subsequently exposed to 0.1 M NaOH solution for 120 min at 80°C.

The formation of copper sulfide layers on PA6 film surface was carried out in two stages. In the first stage, the PA6 films were sulfurized by molten sulfur at 135°C for 1 min in a glass reactor. In the second stage, the samples of sulfurized PA6 films were treated with the aqueous 0.4 M  $\text{CuSO}_4$  solution with the reducing agent at 80°C for 10 min. The PA6 substrate

was placed vertically. After the treatment with the solution of Cu(I/II) salts, the samples of PA6 were rinsed and dried in a desiccator.

### 2.3. Characterization of PA6 and copper sulfide layers

An X-ray diffractometer (D8 Advance diffractometer, Bruker AXS, Karlsruhe, Germany) has been applied to examine the crystal phase of the PA6 and PA6/Cu<sub>x</sub>S samples. The samples were scanned over the range  $2\theta = 3\text{--}70^\circ$  at a scanning speed of  $6^\circ \text{min}^{-1}$  using a coupled two theta/theta scan type. The peaks obtained were identified based on those available in the PDF-2 database.

The optical properties of the PA6 and PA6/Cu<sub>x</sub>S samples were measured at room temperature by using UV/VIS spectrometer Lambda 35 UV/VIS (Perkin Elmer, USA) in the range of 200 to 1100 nm.

The FTIR spectra were recorded in the wavenumber range of 3500 to 600  $\text{cm}^{-1}$  using the compensation method on Perkin Elmer FTIR Spectrum GX 2000 spectrophotometer by averaging 64 scans with a wavenumber resolution of 1  $\text{cm}^{-1}$  at room temperature.

The constant current resistivity of the copper sulfide films was measured using a multimeter MS8205F (Mastech, China) with special electrodes. The electrodes were produced from two nickel-plated copper plates with a 1 cm spacing and the dielectric material between them.

## 3. Results and Discussion

### 3.1. X-ray diffraction analysis

Polyamide 6 has the repeating group  $[-\text{NH}(\text{CH}_2)_5(\text{CO})-]$  and is characterized by the presence of secondary amide groups CO-NH in the polymer skeleton. The hydrogen bonds formed between neighbouring chains strongly affect the mechanical properties. PA6 is semicrystalline; it consists of crystalline and amorphous phases. The degree of crystallinity of PA6 is 35-45 %. The crystalline regions contribute to the hardness, temperature stability, and chemical resistance. Amorphous areas contribute to the impact of resistance and high elongation [31,32]. PA6 has two well-established crystalline modifications of  $\alpha$  phase and  $\gamma$  phase, which can be transformed into each other under certain conditions. The stable monoclinic  $\alpha$  phase is dominant in the structure of PA6; while  $\gamma$  form is unstable, and it can be transformed into the  $\alpha$  form [33].

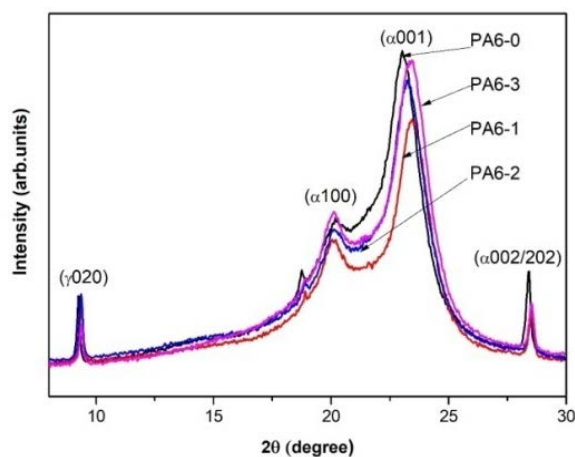


**Fig. 1.** XRD patterns of PA6.

The first task of our work was to study the influence of the polymer preparation on the formation of the copper sulfide thin films by XRD and FTIR analysis.

The XRD diffraction patterns of the initial polyamide films used in the experiments are presented in Fig. 1.

The experimental values of  $d$  (lattice spacing) for the polymer are determined using Bragg's relation [34] by taking the  $\theta$  value from the peak position of XRD pattern:

$$n\lambda = 2d \sin \theta \quad (1)$$

where  $n$  (an integer) is the order of diffraction;  $\lambda$  is the wavelength of incident X-rays;  $d$  is the interplanar spacing of the crystal and  $\theta$  is the angle of incidence. Calculated values of  $d$  are shown in Table II.

**Tab. II** The  $2\theta$ ,  $d$  and  $(hkl)$  Miller indices values of PA6.

$(hkl)$	PA6-0		PA6-1		PA6-2		PA6-3	
	$2\theta$ (°)	$d$ (Å)						
( $\gamma$ 020)	9.24	9.56	9.38	9.42	9.36	9.44	9.36	9.44
( $\alpha$ 100)	20.19	4.39	20.05	4.42	20.11	4.41	20.11	4.41
( $\alpha$ 001)	23.03	3.85	23.44	3.79	23.25	3.82	23.44	3.79
( $\alpha$ 002/202)	28.41	3.14	28.52	3.13	28.52	3.13	28.52	3.13

The peaks of semicrystalline PA6 between  $8^\circ$  to  $30^\circ$  (in  $2\theta$ ) were observed. These peaks, according to JCPDS 12-923, appear at  $\sim 20.1^\circ$  and  $\sim 23.4^\circ$  with the corresponding  $d$ -spacing of  $\sim 4.4$  and  $\sim 3.8$  Å, respectively. They are attributed to the  $\alpha$ 100 and  $\alpha$ 001 crystal planes, respectively, and showed the presence of the dominant crystalline  $\alpha$ -phase [30,32]. Two reflections are also observed at around  $2\theta = 9.3^\circ$  ( $\gamma$ 020) and  $28.5^\circ$   $\alpha$ 002/202.

It has been observed that the intensities and full width at half-maximum (FWHM) values of these peaks slightly changed with the preparation of the PA6 before the formation of the copper sulfide thin films. These changes may be attributed to the crystallinity of the films. The structural parameters for the ( $\alpha$ 001) peak such as FWHM ( $\beta$ ), crystallites size ( $D$ ), dislocation density ( $\delta$ ) and strain ( $\varepsilon$ ) for all the prepared films were evaluated from XRD patterns and presented in Table III. The grain size of the thin films was calculated by XRD patterns using Debye Scherrer's formula [35]:

$$D = \frac{0.9\lambda}{\beta \cos \theta} \quad (2)$$

where  $D$  is the crystallite size;  $\lambda$  is the X-ray wavelength used;  $\beta$  is the angular line width at half-maximum intensity in radians and  $\theta$  is Bragg's angle.

Additionally, to have more information on the number of defects in the films, the dislocation density ( $\delta$ ) was evaluated using the formula [36]:

$$\delta = \frac{1}{D^2} \quad (3)$$

The strain values were calculated from the following relation [37]:

$$\varepsilon = \frac{\beta \cos \theta}{4} \quad (4)$$

The results in Table III showed that the highest value of crystallite size has the polymer PA6-1, while its dislocation density and strain have the lowest value. The larger  $D$ , and the smaller  $\beta$ ,  $\delta$  and  $\varepsilon$  values indicate better crystallization of the films [38,39].

**Tab. III** The crystallite size ( $D$ ), dislocation density ( $\delta$ ), strain ( $\varepsilon$ ) and full width at half maximum (FWHM,  $\beta$ ) values of copper sulfide thin films.

	$2\theta$ (°)	$\beta$ (°)	$D$ (nm)	$\delta \cdot 10^{-2}$ (nm <sup>-2</sup> )	$\varepsilon \cdot 10^{-3}$ (nm <sup>-2</sup> )
<b>PA6-0</b>	23.03	2.61665	30.98	10.42	11.19
<b>PA6-1</b>	23.44	2.2013	36.86	7.36	9.40
<b>PA6-2</b>	23.25	2.42247	33.48	8.92	10.35
<b>PA6-3</b>	23.44	2.22641	35.69	7.85	9.71

X-ray diffraction analysis of the sulfurized PA6 films showed that elemental hexagonal sulfur was diffused into PA6 surface. The peaks of PA6-0 at 9.27°, 18.78°, 20.07°, 23.1°, and 28.4° are attributed to sulfur S<sub>6</sub> [JCPDS No. 72-2402].

XRD studies of Cu<sub>2</sub>S thin films are limited by the polycrystallinity of the layers obtained and by the semicrystallinity of the PA6 film itself. The intensity of the peak maximum of PA6 at  $2\theta < 25^\circ$  exceeds few times the intensity of the copper sulfide peaks maxima. The XRD spectrum recorded after treatment of sulfurized PA6-0 film in Cu(I/II) salt solution shows the peaks at 9.37° (attributed to sulfur), 20.22°, 23.24° and 28.5° (attributed to copper sulfide phase) and indicates the formation of chalcocite, Cu<sub>2</sub>S [JCPDS No. 12-227]. Although the overlapping of XRD peaks makes their identification difficult, the XRD data for other sulfurized and treated samples with copper sulfate solutions are presented in Table IV. They indicate that the composition of Cu<sub>2</sub>S layers does not depend on the pre-treating method of the polymer surface.

**Tab. IV** Comparison of  $d$ -spacing, angle values and their respective planes for Cu<sub>2</sub>S layers obtained by different pre-treating methods of polyamide surface.

	PA6-0		PA6-1		PA6-2		PA6-3		$(hkl)$
	$2\theta$ (°)	$d$ (Å)							
<b>S</b> (hexagonal) JCPDS No 72-2402	9.27	9.53	9.27	9.54	9.27	9.54	9.31	9.49	(100)
	18.78	4.72	18.76	4.72	18.76	4.72	18.83	4.71	(200)
	20.07	4.42	20.14	4.4	20.14	4.4	20.05	4.4	
	23.1	3.85	22.95	3.87	22.95	3.87	23.3	3.8	(101)
	28.4	3.14	28.41	3.14	28.41	3.14	28.5	3.13	(300)
<b>Cu<sub>2</sub>S</b> (orthorhombic) JCPDS No 12-227	20.22	4.39	20.12	4.41	20.12	4.41	20.03	4.43	(212)
	23.24	3.82	23.20	3.83	23.20	3.83	23.3	3.81	(133)
	28.5	3.13	28.54	3.13	28.54	3.13	28.48	3.14	(351)

### 3.2. FTIR spectrum analysis

The FTIR spectra of PA6 films are shown in Fig. 2. PA6 has IR active bands: the stretching band of N–H at about  $\sim 3295$  cm<sup>-1</sup>; at  $\sim 3077$  cm<sup>-1</sup> due to the first overtone of amide II; the symmetrical and asymmetrical stretching bands of a methylene group (CH<sub>2</sub>) at  $\sim 2862$  and  $\sim 2932$  cm<sup>-1</sup>, respectively. The band at  $\sim 1635$  cm<sup>-1</sup> corresponds to the stretching of the amide carbonyl and the one at  $\sim 1537$  cm<sup>-1</sup> is due to the amide II (N–H) in plane bending and C–N stretching [40,41]. In the 650–1400 cm<sup>-1</sup> region of the IR spectra, the modes attributed to CH<sub>2</sub> sequences ( $1478$  cm<sup>-1</sup> – CH<sub>2</sub> scissor vibration,  $1373$  cm<sup>-1</sup> – amide III and CH<sub>2</sub> wag vibration,  $1199$  cm<sup>-1</sup> – CH<sub>2</sub> twist-wag vibration,  $959$  cm<sup>-1</sup> CO–NH in plane

vibration) and crystalline forms of PA6 films can be distinguished. This confirms that the sample studied consists predominantly of  $\alpha$  crystalline form.

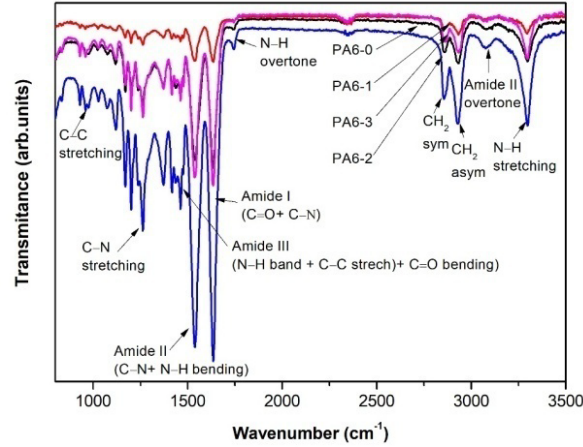


**Fig. 2.** FTIR spectra of PA6.

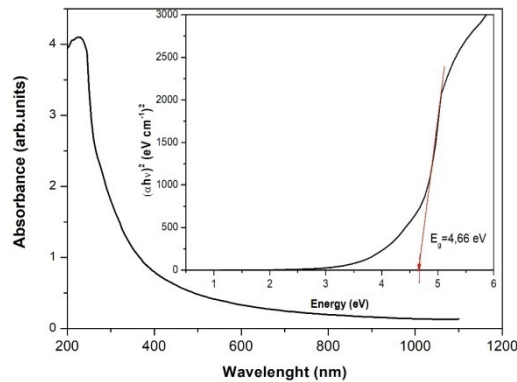
All peaks are consistent with the data in the literature [40,42], but the peak intensities differ when PA6 samples are prepared differently. More intensive peaks were obtained by the treatment of PA6 with an alkali solution. However, no significant differences were observed between the spectra of the PA6-0 and PA6-1, PA6-2, or PA6-3. There were no changes in the shape of these peaks compared to the PA6-0 sample.

### 3.3. UV-VIS absorption spectroscopy

The UV-VIS absorption spectroscopy is a powerful tool for the investigation of the optical properties of the material. In this study we used Tauc plot for the determination of optical band gap from absorbance measurements [43]:

$$\alpha h\nu = A(h\nu - E_g)^n \quad (5)$$

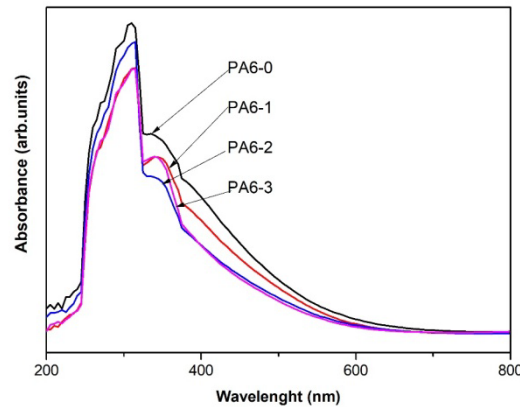
where  $\alpha$  is the absorption coefficient;  $h\nu$  – photon energy;  $E_g$  – energy band gap;  $A$  – a constant;  $n$  – a constant for a given transition ( $n=2$  for direct transition and  $n=1/2$  for indirect transition). The optical band gap can be estimated by extrapolating the linear portion of the  $(\alpha h\nu)^2$  and, respectively  $(\alpha h\nu)^{1/2}$  plots versus  $h\nu$  to  $\alpha = 0$  [44].



**Fig. 3.** UV-VIS absorbance spectrum and plot of  $(\alpha h\nu)^2$  against  $h\nu$  for PA6-0 film (inset).

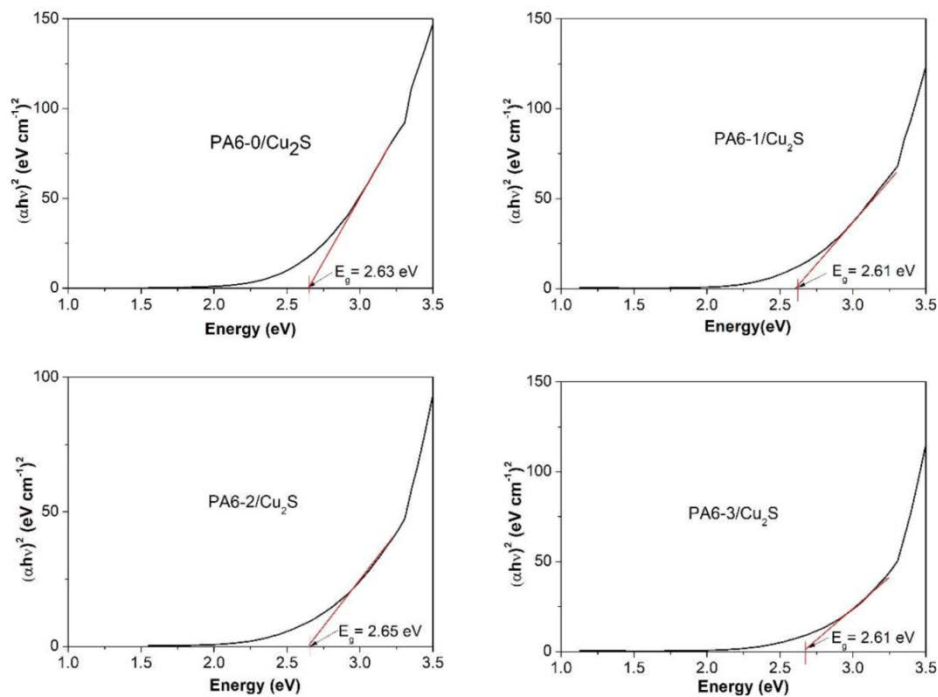
The energy band gap for pure PA6 is 4.66 eV (Fig. 3), which means that the polymer is an insulator. The variations in UV-VIS absorbance spectra of PA6 boiled in distilled water, exposed to a NaOH solution, and boiled in distilled water for 120 min and subsequently exposed to a NaOH solution for 120 min at 80°C are not pronounced in the shape compared to unaterated polyamide 6.

Fig. 4 illustrates that copper sulfide films show strong absorption in the UV region (maximum at cca 320 nm with a shoulder at cca 350 nm) while in the VIS region the absorbance drastically drops.



**Fig. 4.** UV-VIS absorbance spectra of PA6/Cu<sub>2</sub>S films.

Both direct- and indirect-allowed transitions are exhibited in the Cu<sub>2</sub>S film. The experimentally determined values of energy gaps for Cu<sub>2</sub>S thin films slightly differ, their values range from 2.61 to 2.67 eV for direct transitions (Fig. 5), and from 1.40 to 1.44 eV in the case of indirect transitions (Fig. 6). It seems that despite the way the samples of polymer were treated prior to deposition, their optical properties, such as band gap energies, are quite similar.



**Fig. 5.** Plot of  $(\alpha hv)^2$  against  $hv$  for PA6/Cu<sub>2</sub>S films (Direct transition).

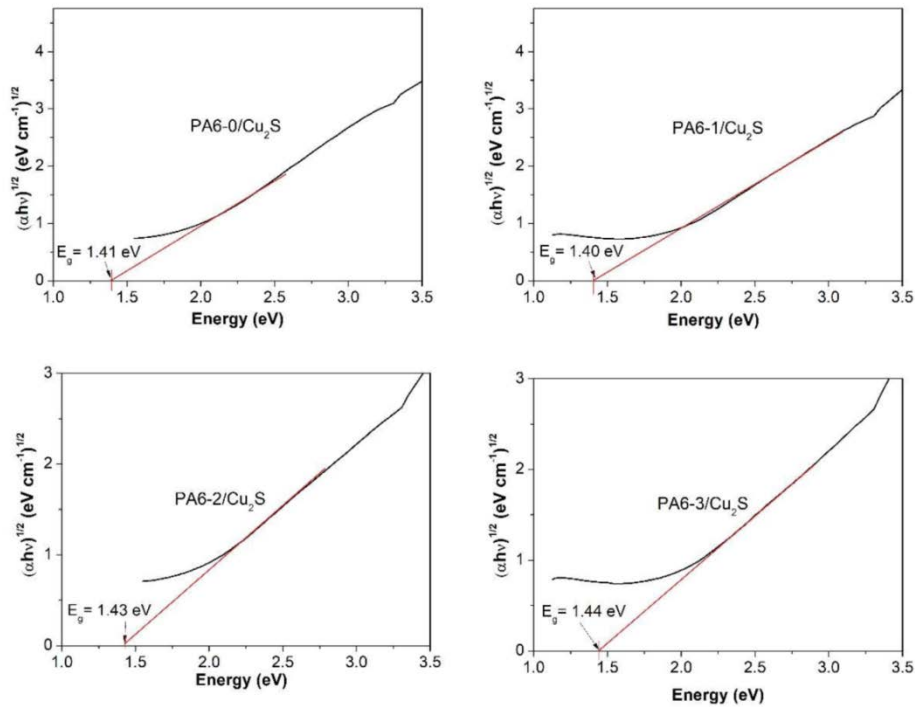


**Fig. 6.** Plot of  $(\alpha hv)^2$  against  $hv$  for PA6/Cu<sub>2</sub>S films (Indirect transition).

In the literature [6,45,46], we can see that the values obtained for  $E_g$  by different authors were not exactly the same: the energy band gap values for Cu<sub>2</sub>S vary from 1.0 to 1.5 eV for indirect transitions and from 2.40 to 2.96 eV for direct transitions. Different values of the energy gap may be due to different techniques of preparation, the thickness of the films obtained, the particle size, and the mechanism of light absorption in the film.

Table V gives the values of the energy gaps obtained in the present work. These results are consistent with the literature [6,45,46].

**Tab. V** The band gap energies of copper sulfide thin films deposited on polymer.

	PA6-0/Cu <sub>2</sub> S	PA6-1/Cu <sub>2</sub> S	PA6-2/Cu <sub>2</sub> S	PA6-3/Cu <sub>2</sub> S
Direct transition (eV)	2.63	2.61	2.65	2.67
Indirect transition (eV)	1.41	1.40	1.43	1.44

The lowest band gap result was obtained for PA6-1/Cu<sub>2</sub>S. A lower bandgap implies higher intrinsic conductivity, i.e. as the energy band gap decreases, the electrical conductivity increases. Therefore, the optical constants were calculated just for PA6-1/Cu<sub>2</sub>S film. As mentioned above, this film has also the best crystallinity.

The optical constants of Cu<sub>2</sub>S thin films were studied using optical absorption theory [6]. According to the conservation law of energy theory, the relation between reflectance ( $R$ ), transmittance ( $T$ ), and absorbance ( $A$ ) is:

$$R+T+A=1 \quad (6)$$

where transmittance ( $T$ ) was measured by  $T = 10^{(-A)}$ . Additionally, the optical constants of Cu<sub>2</sub>S thin films such as the refractive index ( $n$ ) and the extinction coefficient ( $k$ ) are important parameters for thin films. The extinction coefficient ( $k$ ) is the attenuation per unit radiation, and it is related to the absorption coefficient by the following relation:

$$k = \frac{\alpha\lambda}{4\pi} \tag{7}$$

The refractive index ( $n$ ) is the measure of how fast light propagates through the material. The higher the refractive index is, the slower light travels through the material, which changes its direction. It is a very important optical property in designing optical devices. There are many ways to determine the refractive index of the material. In this work, the approach of H. Pathan et al. is used [6]:

$$n = \frac{1 + \sqrt{R}}{1 - \sqrt{R}} \tag{8}$$

The plots of absorbance ( $A$ ), reflectance ( $R$ ) and transmittance ( $T$ ) against wavelength ( $\lambda$ ) (a) and plots of refractive index ( $n$ ) and extinction coefficient ( $k$ ) against  $h\nu$  (b) for PA6-1/Cu<sub>2</sub>S thin film are shown in Fig. 7.

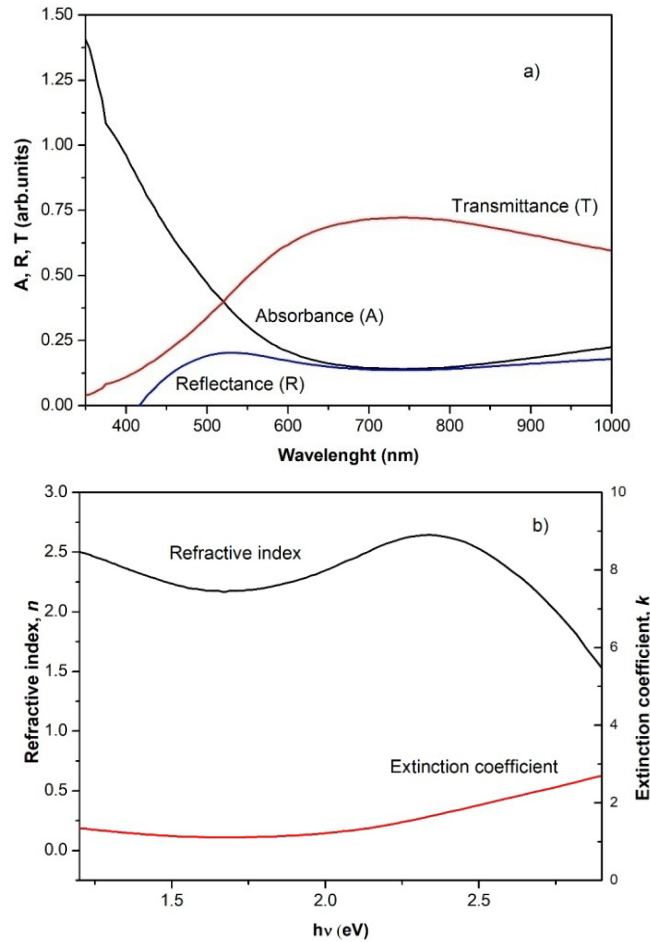


**Fig. 7.** Plots of absorbance ( $A$ ), reflectance ( $R$ ) and transmittance ( $T$ ) against wavelength ( $\lambda$ ) (a) and plots of refractive index ( $n$ ) and extinction coefficient ( $k$ ) against  $h\nu$  (b) for PA6-1/Cu<sub>2</sub>S thin film.

The refractive index value exhibits a minimum at  $\sim 2.17$  for the PA6-1/Cu<sub>2</sub>S thin film at the energy equal to 1.68 eV. The extinction coefficient of the Cu<sub>2</sub>S thin film at the same energy was found to be 0.11.

The real ( $\epsilon_r$ ) and the imaginary ( $\epsilon_i$ ) part of dielectric constant for the same film were determined using the relations [6]:

$$\epsilon_r = n^2 - k^2, \quad (9)$$

$$\epsilon_i = 2nk. \quad (10)$$

The obtained results were shown in Fig. 8.

The imaginary part confirms the contribution of the free carrier to the absorption. From Fig. 7 and Fig. 8 it can be seen that the real and imaginary dielectric constants have the same behaviour as the refractive index and extinction coefficient.

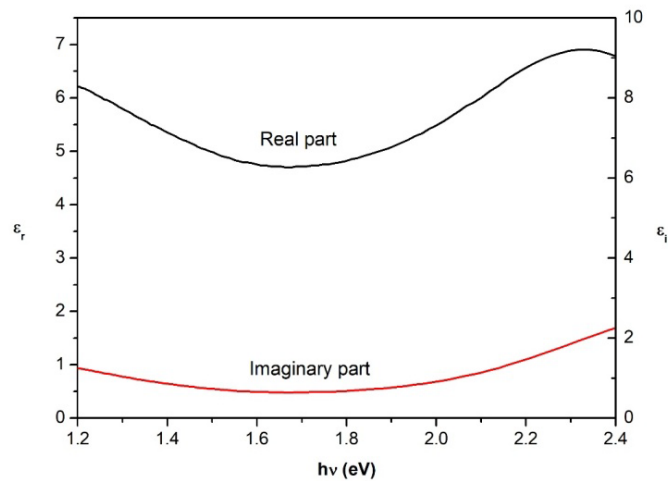


**Fig. 8.** Plot of real ( $\epsilon_r$ ) and the imaginary ( $\epsilon_i$ ) part of the dielectric constant against  $h\nu$  for PA6 - 1/Cu<sub>2</sub>S thin film.

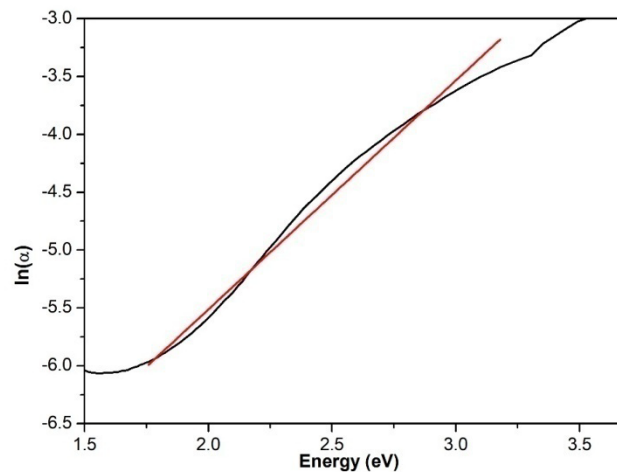


**Fig. 9.** Plot of  $\ln(\alpha)$  against  $h\nu$  for PA6-1/Cu<sub>2</sub>S thin film.

The defect states in the optical band gap region are represented by Urbach energy, which can be extracted from absorption spectra and can be calculated using the following relation [47,48]:

$$\alpha = \alpha_0 \exp\left(\frac{E}{E_u}\right), \quad (11)$$

where  $\alpha$  is the absorption coefficient;  $\alpha_0$  is constant;  $E$  is the incident photon energy which is equal to  $h\nu$ , and  $E_u$  is the Urbach energy. The Urbach energy can be obtained from the slope of the straight line of plotting  $\ln(\alpha)$  against the incident photon energy  $h\nu$ . Fig. 9 shows the variation of  $\ln(\alpha)$  versus  $h\nu$  for the PA6-1/Cu<sub>2</sub>S film.

The Urbach energy value was calculated from the reciprocal of the straight line slope of PA6-1, with the obtained value of 0.51 eV.

The optical conductivity ( $\sigma$ ) was determined using the relation [46]:

$$\sigma = \frac{\alpha n c}{4\pi} \quad (12)$$

where  $\alpha$  is the absorption coefficient;  $n$  is the refractive index of the film, and  $c$  is the speed of light in a vacuum. Fig. 10 shows the variation of optical conductivity ( $\sigma$ ) with energy. The increased optical conductivity is due to the high absorbance of the copper sulfide thin film.

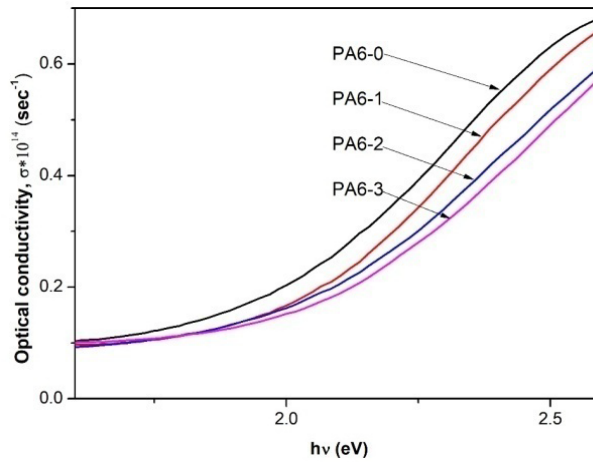


**Fig. 10.** Plot of optical conductivity ( $\sigma$ ) against  $h\nu$  for PA6/Cu<sub>2</sub>S thin film.

The parameters determined for the thin films were compared to those published for Cu<sub>2</sub>S thin films prepared by similar techniques, and it was found that the results of optical constants are consistent with the data from the literature [6].

### 3.4. Measurements of electrical resistivity

Formed Cu<sub>2</sub>S layers changed conductivity of PA6: the surface resistance of pure PA6 is  $1.0 \times 10^{12} \Omega/\text{sq}$ . The square sheet resistance measurements of Cu<sub>2</sub>S layers on PA6 matrix showed that the lowest resistivity was obtained on a sample which was formed on PA6-1 (~7 k $\Omega/\text{sq}$ ), next value was for PA6-3 (~10 k $\Omega/\text{sq}$ ), then on PA6-0 (~60 k $\Omega/\text{sq}$ ), and on PA6-2 electrically conductive layers are not formed (6 M $\Omega/\text{sq}$ ).

## 4. Conclusion

Copper sulfide thin films are deposited on a polymer substrate using the novel sorption-diffusion method. XRD analysis has revealed that the crystallinity of the non-treated

PA6 sample is the highest. After the pre-treatment of PA6, the position and intensity of the peaks changed slightly in diffractograms. According to the diffractograms, elemental hexagonal sulfur was diffused into PA6 surface after sulfurization. The XRD pattern indicates that the  $\text{Cu}_x\text{S}$  films possess a structure that matches the orthorhombic crystal system of the chalcocite ( $\text{Cu}_2\text{S}$ ) phase. Direct and indirect allowed transitions are exhibited for  $\text{Cu}_2\text{S}$  thin films with energy band gaps of 2.61–2.67 eV and 1.4–1.44 eV, respectively. The lowest resistance of copper sulfide thin film was found on PA6-1/ $\text{Cu}_2\text{S}$  and equals  $\sim 7 \text{ k}\Omega/\text{sq}$ . It has been proven that films of good quality for optoelectronic application could be produced by implementing a simple and low-cost technique.

## Acknowledgments

Neringa Petrasauskiene: Conceptualization, Methodology, Investigation, Visualization, Writing - original draft. Edita Paluckiene: Data curation, Methodology, Investigation, Validation, Writing – review & editing. Rasa Alaburdaite: Methodology, Investigation, Writing – review & editing. Martina Gilic: Data curation, Validation, Writing – review & editing.

## 5. References

1. N. S. Kozhevnikova, L. N. Maskaeva, V. P. Markov, O. A. Lipina, A. U. Chufarov, M. V. Kuznetsov, *Mater. Chem. Phys.*, 242 (2020) 122447.
2. L. Isac, I. Popovici, A. Enesca, A. Duta, *Energy Procedia*, 2 (2010) 71.
3. I. Grozdanov, M. Najdoski, *J. Solid State Chem.*, 114 (1995) 469.
4. Y. Zhao, C. Burda, *Energy Environ. Sci.*, 5 (2012) 5564.
5. K. R. Nemade, S. A. Waghuley, *Mater. Sci. Semicond. Process.*, 39 (2015) 781.
6. H. M. Pathan, J. D. Desai, C. D. Lokhande, *Appl. Surf. Sci.*, 202 (2002) 47.
7. Y. Du, Z. Yin, J. Zhu, X. Huang, X. J. Wu, Z. Zeng, Q. Yan, H. Zhang, *Nat. Commun.*, 3 (2012) 1.
8. X. Yu, C. Cao, H. Zhu, Q. Li, C. Liu, Q. Gong, *Adv. Funct. Mater.*, 17 (2007) 1397.
9. L. Qiana, J. Maa, X. Tiana, H. Yuan, D. Xiaoa, *Sensors Actuators, B Chem.*, 176 (2013) 952.
10. H. Lee, S.W. Yoon, E.J. Kim, J. Park, *Nano Lett.*, 7 (2007) 778.
11. M. Tanveer, C. Cao, I. Aslam, Z. Ali, F. Idrees, M. Tahir, W.S. Khan, F.K. Butt, A. Mahmood, *RSC Adv.*, 4 (2014) 63447.
12. Z. Cheng, S. Wang, Q. Wang, *B*) 144.
13. Y. Wu, C. Wadia, W. Ma, B. Sadtler, A.P. Alivisatos, *Nano Lett.*, 8 (2008) 2345.
14. D. Majumdar, *J. Electroanal. Chem.*, 880 (2021) 114825.
15. K.P. Ganesan, A.A. Roselin, *Nano-Structures and Nano-Objects.*, 17 (2019) 138.
16. L. Meng, *Mater. Lett.*, 236 (2019) 131.
17. L. Wu, J. Gao, Z. Qin, Y. Sun, R. Tian, Q. Zhang, Y. Gao, *J. Power Sources*, 479 (2020) 228518.
18. S. Roy, J.W. Rhim, L. Jaiswal, *Food Hydrocoll.*, 93 (2019) 156.
19. A.N. Nikam, A. Pandey, G. Fernandes, S. Kulkarni, S.P. Mutalik, B.S. Padya, S.D. George, S. Mutalik, *Coord. Chem. Rev.*, 419 (2020) 213356.
20. *Commun.*, 122 (2020) 108294.
21. M. Nenadovic, D. Kistic, M. Mirkovic, S. Nenadovic, Lj. Kljajevic, *Sci. Sinter.*, 53 (2021) 187.
22. J. Cardoso, O. Gomezdaza, L. Ixtlilco, M.T.S. Nair, P.K. Nair, *Semicond. Sci. Technol.*, 16 (2001) 123.

23. M.T.S. Nair, P.K. Nair, Semicond. Sci. Technol., 4 (1989) 191.
24. A. Galdikas, A. Mironas, V. Strazdiene, A. Setkus, I. Ancutiene, V. Janickis, Sensors Actuators, B Chem., 67 (2000) 76.
25. A. A. Sagade, R. Sharma, I. Sulaniya, J. Appl. Phys. 105 (2009) 043701.
26. Y. He, T. Day, T. Zhang, H. Liu, X. Shi, L. Chen, G.J. Snyder, Adv. Mater., 26 (2014) 3974.
27. V. Janickis, N. Petrašauskiene, S. Žalėnkiene, I. Morkvenaite-Vilkonciene, A. Ramanavicius, J. Nanosci. Nanotechnol., 18 (2018) 604.
28. E. Balciunaite, N. Petrasauskiene, R. Alaburdaite, G. Jakubauskas, E. Paluckiene, Surfaces and Interfaces, 21 (2020) 100801.
29. R. Alaburdaite, E. Paluckiene, Chalcogenide Lett., 15 (2018) 139.
30. S. L. Fávoro, A. F. Rubira, E. C. Muniz, E. Radovanovic, Polym. Degrad. Stab., 92 (2007) 1219.
31. E. Parodi, G.W.M. Peters, L. E. Govaert, Polymers (Basel), 10 (2018) 1.
32. S. S. Banerjee, A. Janke, U. Gohs, G. Heinrich, Eur. Polym. J. 98 (2018) 295.
33. X. Y. Zhao, B.Z. Zhang, J. Appl. Polym. Sci., 115 (2010) 1688.
34. W.H. Bragg, W.L. Bragg, Proc. R. Soc. London. Ser. A, Contain. Pap. a Math. Phys. Character. 88 (1913) 428-438.
35. A.L. Patterson, Phys. Rev., 56 (1939) 978.
36. B. Güzeldir, M. Sallam, Spectrochim. Acta - Part A Mol. Biomol. Spectrosc., 150 (2015) 111.
37. M. Ashraf, S.M.J. Akhtar, A. F. Khan, Z. Ali, A. Qayyum, J. Alloys Compd., 509 (2011) 2414.
38. M. Saadeldin, H. S. Soliman, H.A.M. Ali, K. Sawaby, Chinese Phys. B, 23 (2014) 046803.
39. H. Shashidharagowda, S. Mathad, M. Abbigeri, Sci. Sinter., 53 (2021) 429.
40. J. Maillo, P. Pages, E. Vallejo, T. Lacorte, J. Gacén, Eur. Polym. J., 41 (2005) 753.
41. N. Vasanthan, D. R. Salem, J. Polym. Sci. Part B Polym. Phys., 39 (2001) 536.
42. V. Krylova, N. Dukštienė, Appl. Surf. Sci., 470 (2019) 462.
43. J. Tauc, R. Grigorovici, A. Vancu, Phys. Status Solidi, 15 (1966) 627.
44. M. Petrovic, M. Gilic, J. Cirkovic, M. Romcevic, N. Romcevic, J. Trajic, I. Yahia, Sci. Sinter., 49 (2017) 167.
45. L. Reijnen, B. Meester, A. Goossens, J. Schoonman, Chem. Vap. Depos., 9 (2003) 15.
46. T. Hurma, S. Kose, Optik (Stuttg), 127 (2016) 6000.
47. H. Chamroukhi, Z. Ben Hamed, A. Telfah, M. Bassou, A. Zeinert, R. Hergenröder, H. Bouchriha, Opt. Mater. (Amst), 84 (2018) 703.
48. A. El-Denglawey, M.M. Makhlof, M. Dongol, M.M. El-Nahass, J. Mater. Sci. Mater. Electron., 26 (2015) 5603.

---

**Сажетак:** У овом раду је представљена нова и повољна метода припреме филмова бакар сулфида на полиамиду. Нетретирани, као и претходно третирани РАБ филмови помоћу 3 различите методе (у кључалој води; у раствору NaOH; у кључалој води на у раствору NaOH) су коришћени као супстрати за формирање слојева  $\text{Cu}_2\text{S}$  сорпционо – дифузионом методом. Као сулфоризациони агенс коришћен је топљени сумпор. За карактеризацију структурних, оптичких и електричних особина узорака, али и за праћење промена након сваког ступња третирања, коришћене су XRD, FTIR и UV-VIS технике. Површински отпор слојева  $\text{Cu}_2\text{S}$  зависи од методе третирања полимера и креће се између 7  $\text{k}\Omega/\text{sq}$  и 6  $\text{M}\Omega/\text{sq}$ . На основу UV-VIS мерења одређене су ширине забрањених зона за директне и индиректне прелазе, и крећу се у опсегу 2.61 – 2.67 eV и 1.40 – 1.44 eV респективно. Одређене су и оптичке константе  $n$ ,  $k$  и  $\sigma$ .

---

---

**Кључне речи:** Танки филмови, бакар сулфид, Полиамид 6, Дифракција рендгенског зрачења, Оптичке особине.

---

© 2022 Authors. Published by association for ETRAN Society. This article is an open access article distributed under the terms and conditions of the Creative Commons — Attribution 4.0 International license (<https://creativecommons.org/licenses/by/4.0/>).

